ACTA NEUROBIOLOGIAE EXPERIMENTALIS

Acta Neurobiol Exp 2004, 64: 171-176

Olfactometry in fMRI studies: odor presentation using nasal continuous positive airway pressure

Roland Popp, Monika Sommer, Jürgen Müller and **Göran Hajak**

Department of Psychiatry, University of Regensburg, Universitätsstr. 84, D-93053 Regensburg, Germany

Technical communication

Abstract. We describe a method for generating and presenting olfactory stimuli in functional magnetic resonance imaging (fMRI) studies for humans. The olfactometer is based on principles of air dilution olfactometry and consists of a nasal mask and a nasal Continuous Positive Airway Pressure device, both normally used for patients suffering from obstructive sleep apnea syndrome. The system allows online monitoring and recording of the subject's breathing pattern. Switching between different olfactory conditions can easily be synchronized with the inhalation phase and be controlled by a computer. Besides, switching occurs rapidly and without any optical, acoustic, thermal, or tactile cues for the subject. As an example of implementation we present a fMRI trial of olfaction using pleasant and unpleasant odor stimuli to induce different affective states in healthy subjects. The relatively inexpensive olfactometer is reliable and permits constant odor concentrations during the inherently prolonged imaging studies.

The correspondence should be addressed to R. Popp, Email: roland.popp@bzk.uni-regensburg.de

Key words: olfactometer, olfactory, fMRI

Functional magnetic resonance imaging (fMRI) makes it possible to study brain activity noninvasively during task performances. The magnetic environment of the scanner that hinders the use of electronic devices has challenged the development of methods and equipment to present appropriate stimuli (e.g., beamer projections presenting optical stimuli or headphones using tubes as conductors of acoustic stimuli). Elaborated block-designs also require the recording of behavioral data such as response reactions, response times, or changes in physiological parameters (for technical solutions see Cornelissen et al. 1997, Meinhardt and Müller 2001, Sommer et al. 2003).

For studying effects of olfactory stimuli, functional neuroimaging has gained wide-spread interest during recent years (Brand et al. 2001, Zald and Pardo 2000). Imaging studies of olfaction place special demands on the presentation of odorant stimulants. Above all, no ferrous material may be placed near the magnet bore. In addition, the system should meet specific conditions (Lorig et al. 1999). An olfactometer should provide the following features: (i) multiple odor administration; (ii) no optical, acoustic, thermal, or tactile cues for the subject should occur when switching between odor- and non-odor phase; (iii) the non-odor phase has to consist of pure air without contamination by other odorants, i.e., no contamination of the olfactometer or of the magnetic room; (iv) well standardized odor generation with good replication in repetitive stimulation trials; (v) temporal control over the odor presentation (i.e., odor rise and fall times); (vi) constant concentration of the olfactory stimulants during prolonged fMRI trials; (vii) a clear distinction between signal (odorant presentation) and no-signal (control condition without odor) in block-design fMRI studies; (viii) ease of operation and handling.

Thus, highly sophisticated olfactometers that have been primarily developed for behavioral and electrophysiological studies were adapted to the magnetic environment (Kobal and Kettenmann 1999). In addition, self-made constructions for olfactory testing have been introduced (Lorig et al. 1999, Sobel et al. 1997).

One aspect, however, that has not been stressed sufficiently so far, is the role of the subject's breathing pattern. Imaging studies have revealed that it makes a difference whether subjects inhale or sniff an odorant (Lorig et al. 1996, Sobel et al. 1998). This distinction has to be considered in the planning of the experimental design. When the subject is supposed to continue a regular breathing cycle during odor presentation, the inspiration and expiration phases need to be monitored and recorded carefully. This assures that changes of the cerebal blood flow are solely due to olfactory processing and not caused by a motor response, i.e., by an altered breathing pattern. Furthermore, the monitoring makes it possible to synchronize the onset of the odor presentation with the inhalation phase of the subject, which is critical for olfactory perception. This prevents unwanted delay of odor detection after stimulus onset, which may last up to several seconds. Finally, it is useful to receive feedback regarding the subject's air flow in order to detect clinically relevant changes of respiratory parameters (e.g., hyper- or hypoventilation).

The research instrument described here meets the above mentioned demands and goes beyond their scope by the integrated capacity to monitor the amplitude and the frequency of the subject's breathing activity. We modified a nasal mask and a Continuous Positive Airway Pressure (CPAP) device, both normally used to alleviate patient suffering from obstructive sleep-related breathing disorders (Sullivan et al. 1981). The odor generation unit is based on principles of air dilution olfactometry and consists of off-the-shelf pneumatic parts and standard laboratory equipment. Thus, the apparatus can be easily constructed in a cost-effective manner.

The odor generation unit consists of saturation bottles with odor samples, valve switching devices, a carrier air stream and a flowmeter to control the flow rate. The odor stimuli are generated by an air stream that passes over the odor samples.

In our study, compressed air for the olfactometer was supplied by the air compressing system of the medical institute. Alternatively, an air compressor may serve the same purpose. The compressed air is purified by a filter of activated charcoal. The pressure of the odor-free air stream is regulated by a valve and its flow rate is controlled by a flowmeter (Rota GmbH, Germany; for constant flow rates of 2,000 ml/min). All connecting tubing is odorless and very resistant to pressure, as they are normally used in pneumatic systems (e.g., Festo, Germany; 6 mm diameter).

By means of a pneumatic three-way valve-switching device (Festo, Germany), which is controlled by a computer, different odor and no-odor conditions can be chosen by routing the air stream to various odor chambers *via* 8 m long tubes. For the switching device we used three 100 ml gas washing bottles (Merck Eurolab GmbH, Germany), which allowed the application of two different odor stimuli and one control. Due to the

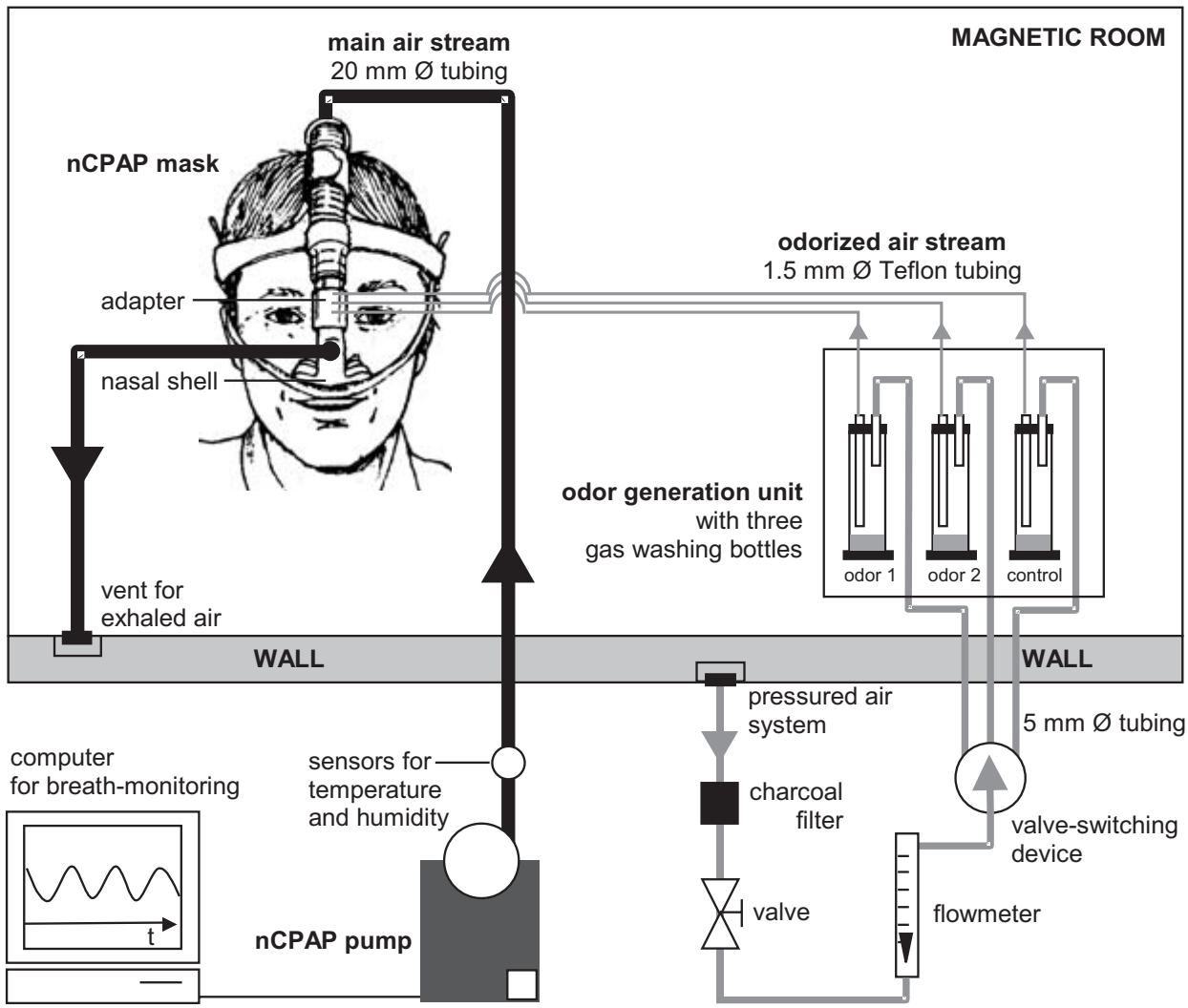

Fig. 1. Schematic diagram for the presentation of olfactory stimulants. See the text for explanations.

excess pressure in the tubing system, the top part of all bottles were fixed by plastic clips. As the odor generation unit did not contain any ferrous metal, the bottles could be placed close to the subject within the magnetic room.

The air passes through one of the 100 ml gas washing bottles filled with different odorant solutions. One bottle containing only the non-odorous solvent (e.g., distilled water) is used as a control. Molecules of odorants that are in the vapor phase over the surface of the solution ("headspace") diffuse into the air stream and are then replaced by further evaporation into the headspace (for diffusion method of air dilution olfactometry see Prah et al. 1995). In our experimental setting, each bottle contained 2 ml aqueous solution. A sufficient amount of odorant solutions ensures a steady output and constant odor concentration over the inherently long duration of fMRI study trials, which can be a problem for other self-made olfactometers.

For odor application the odorized air is mixed with a neutral, continuous main air stream. Therefore, the odorized carrier air stream from the bottle is passed *via* 150 mm long, only 2 mm inner width Teflon tubing (DuPont ™) to a modified nasal CPAP-mask on the subject's nose (Adam CPAP Circuit ™, MAP, USA).

The odorless main air stream is produced by a CPAP pump (Selfset ™, MAP, USA) placed outside of the magnetic room. The air is passed directly *via* 8 m long, 20 mm diameter tubes to the nasal mask. The mask consists of a nasal shell and two nasal Silicon pillows, which are inserted into the nostrils. The CPAP mask is attached to a headgear to keep it in place and fixed by a shell strap on

the subject's head (SnugFit™, MAP, USA). The nasal pillows must seal at the nostrils securely.

The connection between all odor-tubing and the adapter for the ADAMS-mask is air-tight. Within the circuit the odorant air mixes with the main air stream before entering the muscoa. So far, the design of the mask only allows birhinal stimulation. The volume of the nasal shell is relatively low (ca. 25 ml) accounting for a much smaller dead-space volume compared to ordinary CPAP or anesthesia masks (at least 60 ml). The relatively high flow rate of the main air stream allows rapid clearing of the accumulated odorant air immediately after switching from an odor to a non-odor phase. As the inner-space volume of the odor-tubing (150 cm long, only 2 mm inner diam) is also very small, the stimuli can be presented with rapid rise times. Switching between different odor conditions does not provide optical, acoustic, thermal, or mechanical cues for the subject. The odor concentration can be adjusted by changing either the flow rate of the odorized air stream or of the nCPAP device.

The nCPAP circuit complies with the requirements and directives for medical devices.

Nearly all elements which come in contact with odorized air are made either out of glass or Teflon, which reduce the risk of contaminating the system by adherence of the odorants. If necessary, the interior of the mask could also be coated with Teflon.

To prevent the magnet bore from contamination by emitted odorants, we ensured that no exhaled air was released into the magnetic room. To remove the air immediately we positioned a 20 mm diameter Polypropylene tube at the 4 mm bore release-opening for the exhaled air. A 5 m long tube leads to the medical ventilation opening where anesthesia gas is normally drawn off (15 mbar below atmospheric pressure).

The flow rate of the main air stream within the CPAP Circuit is controlled by the pressure of the CPAP pump. (We used 4 mbar as a reference which equals a flow rate of 4 liters per minute in our system). As changes in the nasal mask are constantly measured *via* an additional pressure tube, the pressure remains very stable. Pressure drops are adjusted automatically.

If necessary, the CPAP device makes it possible to warm and humidify the main air stream. We measured its temperature and humidity by electronic sensors inserted into an adapter outside of the magnetic room close to the CPAP unit (temperature: 20-22°C, humidity: 55-60%).

Some auto-adjust CPAPs (e.g., Selfset™ or Magellan™, MAP, Germany) are able to monitor the inspiration-expiration-cycle of a subject online and display the breathing curve on an attached computer. Therefore in fMRI studies, no additional breathing sensor has to be applied to register the airflow or thorax activation of the subject lying in the magnetic bore. The CPAP monitoring easily makes it possible to synchronize the odor application with the inspiration phase of the subject. This prevents a delay of olfactory perception in the range of up to 3 s, if the "odor condition" is accidentally started while the subject is in the expiration phase. The monitoring also serves as feedback system of any unwarranted signs during the experimental setting (e.g., leakage flow, hypo- or hyperventilation of the subject, etc.).

As the frequency and amplitude of the inspiratory airflow can be measured exactly, any variation of the breathing pattern is quite easily detectable (e.g., when a very pleasant or unpleasant odor is applied). This ensures that changes in the brain activity (i.e., changes in the blood oxygen level dependent (BOLD) signal) are not due to motor induced activation, but are caused by altered olfactory processing.

This is especially critical in studies, when subjects are explicitly asked not to sniff, but to inhale the supplied air constantly.

In addition, the CPAP selfset system allows to record and store the raw data of the airflow curves, the CPAP pressure and markers made during the online recordings. A printout can serve as documentation for the course of the experiment.

As an example of technical implementation we present a fMRI trial of olfaction using pleasant and unpleasant odor stimuli to induce different affective states in healthy subjects.

We measured four, non-smoking volunteers during an olfactory fMRI-experiment. The two women (34 and 38 years) and the two men (32 and 39 years) were free from any documented history of serious head injury. All participants were right-handed and gave informed consent prior to data collection.

The fMRI experiment consists of two sessions. Each session was planned as a block design with 3 pleasant (vanillin-solvent 10%, 2 ml, presentation time 10 s) and 3 unpleasant (butyric acid 10%, 2 ml, presentation time 10 s) blocks intermittent with neutral ones (20 s). Every session began with a neutral condition. Before, all participants had rated vanillin as very pleasant and butyric acid as very unpleasant.

Blood oxygenation level-dependent fMRI (BOLD) was acquired with a 1.5 Tesla Siemens Symphony system, (Siemens, Erlangen, Germany) using a gradient echo planar imaging (EPI) sequence. Shimming was optimized with an automated Siemens shim adjust. To prevent head motion, foam pads were placed inside the head coil.

A T_2*-weighted echo planar imaging sequence (100 measurements; TR = 2,092.0 ms; TE = 60 ms; $\alpha = 90°$, in plane matrix 64 × 64; FoV = 240 × 240 mm; slice-thickness = 5.0; distance factor 0.2; pixel size = 3.75 mm × 3.75 mm) was applied with a stack of 20 contiguous slices (5 mm thickness each) aligned to the AC-PC-plane. Except for the most inferior cerebellum, this covered the entire brain. The time period for the acquisition of the 20 slices was 2 s. A total of 100 images was acquired for each subject, with the first four images being discarded in later data processing. For anatomical correlation, a high-resolution T_1-weighted scan was acquired before the fMRI experiment (TR = 11,1 ms, TE = 4,3 ms, $\alpha = 90°$, matrix 256^3, isotropic voxel size 1 mm^3).

Data analysis and visualization were performed using the fMRI software package BrainVoyager 4.6 (BrainInnovation, Maastricht, The Netherlands).

The preprocessing consisted of the following steps: three-dimensional motion correction, slice scan-time correction, trend removal by temporal fast Fourier transform-based high-pass filtering, removing frequency components below 3 cycles within the time series and transformation into Talairach coordinate space.

The statistical analysis is based on the general linear model (GLM). The principal analyses consisted of the comparison between the pleasant and unpleasant odor. Laterality differences could not be calculated due to the small sample size. The time course was modulated with a delayed box-car function convolved with a hemodynamic response function in the context of a general linear model. The results refer to a standard Talairach brain. All results were corrected for serial correlation.

In contrast to the unpleasant odor-stimuli of butyric acid, the pleasant stimuli of vanillin induced significant activation primarily in the left middle frontal gyrus and left superior temporal gyrus (see Table I).

Compared to the pleasant stimuli unpleasant stimuli induced significant activation in the left inferior frontal gyrus, left lingual gyrus, right putamen, anterior cingulate, right transverse temporal gyrus and right praecentral gyrus (see Table I).

The activation of frontal areas by odor-stimulation is in line with results of previous fMRI-research. Kobal and Kettenmann (2000) and Sobel et al. (1997) found increased activation following stimulation with vanillin in different frontal areas. Our results showed specific activation patterns in frontal regions dependent of the valence of stimulation. Pleasant stimulation activated primarily dorsolateral frontal areas (BA 46, BA 9), whereas unpleasant odors led to more activation in the orbitofrontal area (BA 47).

Table I

Activated brain regions while odor stimulation

Condition	Brain region	Center Talairach Coordinates			Size	*t*-value
		x	y	z		
VA>BA	Left middle frontal gyrus (BA46)	-42	47	16	1,600	4.5
	Left middle frontal gyrus (BA 9)	-51	10	35	146	3.5
	Left superior temporal gyrus (BA 22)	-60	-28	18	326	3.6
BA>VA	Left inferior frontal gyrus (BA 47)	-43	25	-11	152	3.5
	Left lingual gyrus (BA 18)	-19	-50	6	153	3.9
	Right putamen	25	-14	7	248	4.2
	Right anterior cingulate	6	38	25	176	2.9
	Left anterior cingulate	-6	39	0	63	3.1
	Right transverse temporal gyrus (BA 41)	35	-23	10	129	3.9
	Right praecentral gyrus	46	-8	33	713	5.0

(VA) vanillin; (BA) butyric acid. The position of each area is given as the Talairach coordinates of the center of mass of supra-threshold clusters ($P<0.01$, corrected for serial correlation) of the group analysis.

In our study vanillin led to significant activation of the left superior temporal gyrus. Odor related activity of this structure was described by Kettenmann et al. (1996) and Kobal and Kettenmann (2000). In primates anatomical connection between the inferior orbitofrontal gyrus, which receives input from olfactory structures, and the superior temporal sulcus were shown (Carmichel and Price 1996).

In contrast to vanillin, the unpleasant odor of butyric acid significantly activated the anterior cingulate cortex (ACC). Odor induced activity of the cingulate was also reported from Levy et al. (1997) and Fulbright et al. (1998). Furthermore, the ACC is a part of the brain`s limbic system and plays a central role in emotion processing (Bush et al. 2000, Phan et al. 2002).

CONCLUSION

The described method for well-standardized olfactory stimulus presentation can be used for various applications. In our pilot study for emotion induction by pleasant and unpleasant odor stimuli, it proved reliable in application of the odor stimuli. The olfactometer system meets all critical demands of olfactory fMRI studies. In addition, it incorporates a breathing monitor function. The instrument can be constructed easily and at low cost from standard pneumatic parts and equipment from sleep medicine.

The apparatus might be helpful to apply olfactometry in fMRI studies, not only for healthy subjects but also for psychiatric patients, e.g., previous imaging studies have demonstrated different functional patterns of brain responses to olfactory stimulation in schizophrenia (Crespo-Facorro et al. 2001).

Brand G, Millot JL, Henquell D (2001) Complexity of olfactory lateralization processes revealed by functional imaging: a review. Neurosci Biobehav Rev 25: 159-166.

Bush G, Luu P, Posner MI (2000) Cognitive and emotional influence in anterior cingulate cortex. Trends Cogn Sci 4: 215-222.

Cornelissen FW, Pelli DG, Farell B, Huckins SC, Szeverenyi NM (1997) A binocular fiberscope for presenting visual stimuli during fMRI. Spat Vision 11: 75-81.

Crespo-Facorro B, Paradiso S, Andreasen NC, O`Leary DS, Watkins L, Ponto LLB, Hichwa RD (2001) Neural mechanisms of anhedonia in schizophrenia. JAMA 286: 427-435.

Fulbright RK, Skudlarski P, Lacadie CM, Warrenburg S, Bowers AA, Gore JC, Wexler BE (1998) Functional MR imaging of regional brain responses to pleasant and unpleasant odors. Am J Neuroradiol 19: 1721-1726.

Kettenmann B, Jousmaki V, Portin K, Samlelin R, Kobal G, Hari R (1996) Odorants activate the human superior temporal sulcus. Neurosci Lett 203: 143-145.

Kobal G, Kettenmann B (1999) Cerebral representation of odor perception. Adv Neurol 81: 221-229.

Kobal G, Kettenmann B (2000) Olfactory functional imaging and physiology. Int J Psychophysiol 36: 157-163.

Levy LM, Henkin RI, Hutter A, Lin CS, Martins D, Schellinger D (1997) Functional MRI of human olfaction. J Comput Assist Tomogr 21: 849-856.

Lorig TS, Elmes DG, Zald DH, Pardo JV (1999) A computer-controlled olfactometer for fMRI and electrophysiological studies of olfaction. Behav Res Methods Instrum Comput 31: 370-375.

Lorig TS, Matia DC, Peszka J, Bryant DN (1996) The effects of active and passive stimulation on chemosensory event-related potentials. Int J Psychophysiol 23: 199-205.

Meinhardt J, Müller J (2001) Motor response detection using fiber optics during functional magnetic resonance imaging. Behav Res Methods Instrum Comput 33: 556-558.

Phan KL, Wager T, Taylor SF, Liberzon I (2002) Functional neuroanatomy of emotion: A meta-analysis of emotion activation studies in PET and fMRI. Neuroimage 16: 331-348.

Prah JD, Sears SB, Walker JC (1995) Modern approaches to air dilution olfactometry. In: Handbook of olfaction and gustation (Ed. R. Doty). New York, Marcel Dekker, p. 227-256.

Sobel N, Prabhakaran V, Desmedt JE, Glover GH, Sullivan EV, Gabrieli JDE (1997) A method for functional magnetic resonance imaging of olfaction. J Neurosci Methods 78: 115-123.

Sobel N, Prabhakaran V, Desmond JE Glover GH, Goode RL, Sullivan EV, Gabrieli JD (1998) Sniffing and smelling: separate subsystems in the human olfactory cortex. Nature 392: 282-286.

Sommer M, Meinhardt J, Volz H-P (2003) Combined measurement of event-related potentials (ERPs) and fMRI. Acta Neurobiol Exp (Wars) 63: 49-53.

Sullivan CE, Issa FG, Berthon-Jones M, Eves L (1981) Reversal of obstructive sleep apnea by continious positive airway pressure applied through the nares. Lancet 1: 862-865.

Zald DH, Pardo JV (2000) Functional neuroimaging of the olfactory system in humans. Int J Psychophysiol 36: 165-181.

Received 22 December 2003, accepted 23 March 2004